

Chemical reaction dynamics of Rydberg atoms with neutral molecules: A comparison of molecular-beam and classical trajectory results for the $H(n)+D_2 \rightarrow HD+D(n')$ reaction

Hui Song, Dongxu Dai, and Guorong Wu

State Key Laboratory of Molecular Reaction Dynamics, Dalian Institute of Chemical Physics, Chinese Academy of Sciences, Dalian, Liaoning 116023, People's Republic of China

Chia Chen Wang

Department of Chemistry, University of California at Berkeley, Berkeley, California 94620

Steven A. Harich

State Key Laboratory of Molecular Reaction Dynamics, Dalian Institute of Chemical Physics, Chinese Academy of Sciences, Dalian, Liaoning 116023, People's Republic of China

Michael Y. Hayes

Department of Chemistry, University of Colorado at Boulder, Boulder, Colorado 80309

Xiuyan Wang

State Key Laboratory of Molecular Reaction Dynamics, Dalian Institute of Chemical Physics, Chinese Academy of Sciences, Dalian, Liaoning 116023, People's Republic of China

Dieter Gerlich

Institute für Physik, Technische Universität Chemnitz, 09107 Chemnitz, Germany

Xueming Yang

State Key Laboratory of Molecular Reaction Dynamics, Dalian Institute of Chemical Physics, Chinese Academy of Sciences, Dalian, Liaoning 116023, People's Republic of China

Rex T. Skodje^{a)}

Department of Chemistry, University of Colorado at Boulder, Boulder, Colorado 80309 and Institute of Atomic and Molecular Sciences, Academia Sinica, P.O. Box 23-166, Taipei, Taiwan

(Received 16 May 2005; accepted 21 June 2005; published online 23 August 2005)

Recent molecular-beam experiments have probed the dynamics of the Rydberg-atom reaction, $H(n)+D_2 \rightarrow HD+D(n)$ at low collision energies. It was discovered that the rotationally resolved product distribution was remarkably similar to a much more limited data set obtained at a single scattering angle for the ion-molecule reaction $H^++D_2 \rightarrow D^++HD$. The equivalence of these two problems would be consistent with the Fermi-independent-collider model (electron acting as a spectator) and would provide an important new avenue for the study of ion-molecule reactions. In this work, we employ a classical trajectory calculation on the ion-molecule reaction to facilitate a more extensive comparison between the two systems. The trajectory simulations tend to confirm the equivalence of the ion+molecule dynamics to that for the Rydberg-atom+molecule system. The theory reproduces the close relationship of the two experimental observations made previously. However, some differences between the Rydberg-atom experiments and the trajectory simulations are seen when comparisons are made to a broader data set. In particular, the angular distribution of the differential cross section exhibits more asymmetry in the experiment than in the theory. The potential breakdown of the classical model is discussed. The role of the “spectator” Rydberg electron is addressed and several crucial issues for future theoretical work are brought out. © 2005 American Institute of Physics. [DOI: 10.1063/1.1998807]

I. INTRODUCTION

The collisions of the highly excited Rydberg atoms (RAs) with neutral atoms and molecules have been studied for many years.^{1,2} It is well appreciated that the physical characteristics of RA collisions differ greatly from their ground-state counterparts.³ Indeed, the energy-level spacing between high- n Rydberg states is generally much smaller

than typical translational collision energies, thus signaling a breakdown of the conventional Born-Oppenheimer picture. Furthermore, time and length scales of RA collisions are extremely different from those for “typical” atom-molecule systems. Indeed, the Bohr radius of the high- n Rydberg electron ($r_n \sim 2000a_0$ for $n=50$) is vastly larger than the scattering length for the collision while the classical orbit period ($\tau_n \sim 20$ ps for $n=50$) is far greater than the nominal collision time. To understand such systems, Fermi⁴ proposed an “independent-collider” model, in which the (Rydberg)

^{a)}Electronic mail: skodje@spot.colorado.edu

electron+target and ion-core+target scattering events were treated independently in the overall collision of RA with atoms or molecules. Fermi's independent-collider model has proven successful in interpreting the results for a number of experiments involving RA collisions, and has served as the starting point for a variety of theoretical models.^{3,5-8} Most studies of RA+molecule collisions thus far have focused on processes that are dominantly mediated through electron+target component of the scattering, such as near resonant electronic-to-rotational energy transfer or collision-induced ionization.^{3,9-11} There have been relatively few studies that probe events sensitive to the ion-core+molecule scattering event,^{5,6} and even fewer that were carried out at a fully state resolved level. Recently, however, Strazisar *et al.*¹² have studied the vibration excitation of N₂ and O₂ molecules in collisions with high-*n* H-RA which was dominated by the ion-core+molecule scattering event.

Of interest here are chemically reactive RA+molecule collisions occurring at relatively low collision energies, $E_C < 1.5$ eV. In the present work we investigate the chemical reaction



where $n(n')$ denote the initial (final) principal quantum number of the Rydberg electron while (νj) are the vibration and rotational quantum numbers. Chemical reactions have been observed previously in RA+molecule scattering, e.g., $\text{K}(np) + \text{CCl}_4 \rightarrow \text{K}^+ + \text{CCl}_3 + \text{C}^-$,¹³ and are often initiated by an electron transfer event that forms an intermediate anion. Here, since the D_2^- species does not exist, we expect reaction (1) to occur through the direct interaction of the H^+ ion core with the D_2 species. Thus, the simplest view of this reaction consistent with Fermi's independent-collider model is that of an ion-molecule reaction,



where the Rydberg electron merely acts as a spectator during the course of the collision. The focus of the present work is the quantitative connection between the two collision processes, (1) and (2). If the Rydberg electron were truly an inessential spectator to the reaction dynamics, then we might expect a relationship between the differential cross sections (DCSSs) of the form

$$\begin{aligned} & \frac{d\sigma[\text{H}^+ + \text{D}_2(\nu, j) \rightarrow \text{HD}(\nu', j') + \text{D}^+]}{d\Omega} \\ & \approx \sum_{n'} \frac{d\sigma[\text{H}(n) + \text{D}_2(\nu, j) \rightarrow \text{HD}(\nu', j') + \text{D}(n')]}{d\Omega}, \end{aligned} \quad (3)$$

where $\nu(\nu')$ and $j(j')$ denote the initial (final) vibrational and rotational quantum numbers. If, in fact, Eq. (3) is found to be quantitatively accurate, the practical implications would be significant. This would imply that the ion+molecule reactive scattering process could be studied by considering the analog RA collision. The potential connection between such pairs of problems has been noted before, e.g., by Pratt *et al.*¹⁴ who investigated the $\text{H}_2(n) + \text{H}_2$ system. Ion-molecule reactions

are difficult to study accurately in a molecular-beam experiment since the space-charge repulsion of the ion beam reduces signal and leads to loss of energy resolution. On the other hand, intense beams of (neutral) RA can be produced with well-defined collision energies using now well-established technology.^{15,16}

In a recent report, we have presented the results of an experimental study of reaction (1) carried out using a crossed molecular-beam apparatus.¹⁷ The state-resolved DCS was measured at two collision energies. It was noted that the rotational product distribution obtained was consistent with earlier results for the ion-molecule reaction $\text{H}^+ + \text{D}_2$ that were measured at one scattering angle.¹⁸ Here, we investigate the connection between the experimental $\text{H}(n) + \text{D}_2$ reactive scattering results and a theoretical representation of the ion-molecule reaction $\text{H}^+ + \text{D}_2$. The experiment has provided a fully state-resolved differential cross section, and thus a scattering calculation is required for the $\text{H}^+ + \text{D}_2$ system. While converged numerical quantum scattering calculations have been accomplished for a number of neutral $A + BC$ reactions, ion-molecule reactions present a severe challenge. Long-ranged potential interactions and the generic existence of deep binding wells have thus far restricted accurate quantum calculations to single partial-wave scattering, i.e., zero impact parameter.¹⁹ Recently, however, Last *et al.*²⁰ and Panda and Sathyamurthy *et al.*²¹ have accomplished approximate quantum calculations on $\text{H}^+ + \text{H}_2$ and $\text{He}^+ + \text{H}_2$, respectively. Thus, we adopt the quasiclassical trajectory (QCT) methodology to model the system. While quantum effects will surely play a role in the detailed state and angle distributions of the reaction, the QCT approach has been widely tested and has often been found to yield reasonably good agreement with full quantum scattering calculations, when the latter are available. In fact, various isotopic variations of reaction (1) have been previously studied using QCT on the early versions of the potential-energy surface (PES).^{22,23} However, it is necessary here to perform further QCT calculations to mimic the detailed experimental conditions and to make use of a more accurate PES that is now available.²⁴

The role of the "spectator" Rydberg electron in perturbing the ion-molecule scattering process is obviously an important issue determining the potential validity of Eq. (3). In the QCT calculations here, the Rydberg electron is simply ignored and the results are directly compared to the experimental results for RA+molecule system. However, we can make very elementary estimates of the influence of the electron using classical approximations. As we shall see, it is likely that many of the mechanisms that couple the electron to the nuclear scattering event are small. However, it remains for further work to rigorously decide this issue.

The paper is organized in the following way. In Sec. II, the QCT calculations and the PES are described. Since the methodology of QCT simulations is well known, this discussion is quite brief. In Sec. III, the results of the QCT simulation for the ion-molecule reaction are presented. In Sec. IV, we present a comparison of the theoretical simulations to the available experimental observations. It is concluded that the results are generally consistent with the ion-molecule interpretation of the RA-molecule reaction. However, some dif-

TABLE I. Energetic thresholds.

Channels	Threshold energies	ΔE (eV)
$H^+ + D_2(0,0) \rightarrow H^+ + D_2(0,0)$		0.0
$H^+ + D_2(0,0) \rightarrow H^+ + D_2(1,0)$		0.371
$H^+ + D_2(0,0) \rightarrow D^+ + HD(0,0)$		0.040
$H^+ + D_2(0,0) \rightarrow D^+ + HD(1,0)$		0.450
$H^+ + D_2(0,0) \rightarrow D + HD^+(0,0)$		1.870
$H^+ + D_2(0,0) \rightarrow H^+ + D + D$		4.55

ferences exist that remain to be explained. In Sec. V the potential influence of the Rydberg electron on the outcome of the experiment is considered. The analysis is limited to simple classical estimates but serves to identify important issues for further theoretical research. Section VI presents a summary of the results and the concluding remarks.

II. CLASSICAL TRAJECTORY SIMULATIONS

In this section, we describe the methods used to carry out the QCT simulations of the $H^+ + D_2 \rightarrow HD + D^+$ reaction. For reference, in Table I we provide the energetic thresholds (including zero-point energy) for a number of the possible final channels of the collision. Since the collision energies considered in this study are below 1.5 eV, only the inelastic ($H^+ + D_2(\nu'j')$) and rearrangement ($D^+ + HD$) final channels are open. At low collision energies, we neglect any nonadiabatic coupling in the ion-molecule reaction and the simulations were carried out on a representation of the ground-state potential-energy surface. Kamisaka *et al.*²⁴ recently produced a modified diatomics-in-molecules potential-energy surface (DIM-PES) that has incorporated *ab initio* data through a modification of the original DIM prescription. This KBNN-PES exhibits no barrier to reaction along the T-shaped reaction path, and has a well depth of 4.5 eV at the equilibrium geometry of the HD_2^+ species (an equilateral triangle). In Fig. 1, we plot a contour diagram of the KBNN-PES at T-shaped geometries as a function of R (the distance between H^+ and the center of mass of D_2) and r (the bond length of D_2).

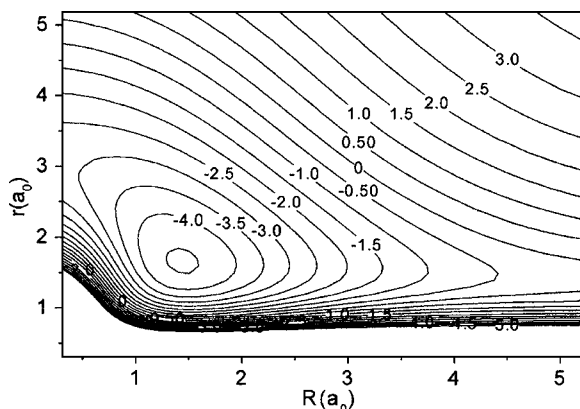


FIG. 1. Contour map of the ground electronic state KBNN-PES of HD_2^+ . The potential energy in eV is plotted as a function of R and r (in a.u.) for the T-shaped geometry. R is the distance between H^+ and the center of mass of D_2 , r is the distance of D_2 .

The methodology of quasiclassical trajectory simulations for atom-diatom reactions is well known^{25,26} and does not require a detailed review. Briefly, the trajectories were propagated using a simple Runge-Kutta integration scheme employing a fixed time step size of 3.5 a.u. This was sufficient to ensure energy conservation of better than five significant figures. The initial conditions were selected to model the $H^+ + D_2(0,0)$ state using the simplest WKB prescription. Specifically, the vibrational action of D_2 , computed from the exact potential, was constrained to be $h/2$ and the initial diatomic rotational angular momentum was taken to be zero. The initial separation, $R(H^+ - D_2)$ was set to be $25a_0$ and the trajectories were propagated until the final product separation again reached $25a_0$. Because of complex formation, the propagation time required was generally quite long (several picoseconds). Each collision energy was modeled using 100 000 trajectories that randomly sampled the vibrational-rotational phases and the impact parameter. The final quantum state of the product diatom was determined in two distinct ways. First, the state distribution was determined using conventional histogram binning of the final vibrational action and diatomic angular momentum. In the second approach, the final state was selected using the Gaussian weighting procedure described by Bonnet and Rayez²⁷ and Banares *et al.*²⁸ For the differential cross sections, smooth angular distributions were obtained by fitting the distribution of scattering angle to an expansion in Legendre polynomials. The calculations were carried out at 14 collision energies in the range $E_C = 0.124 - 1.424$ eV for this system. The main focus is on the case $E_C = 0.524$ eV where the experimental results have been fully analyzed. For this case, 500 000 trajectories were used.

Typical reactive trajectories were found to proceed through a long-lived intermediate complex. To estimate the collisional lifetime, τ , from the total trajectory propagation time, T , we subtract the free asymptotic propagation times to obtain

$$\tau = T - \frac{R_{\text{final}}}{\nu_{\text{final}}} - \frac{R_{\text{initial}}}{\nu_{\text{initial}}}. \quad (4)$$

III. RESULTS OF QCT SIMULATION

The excitation function $\sigma_R(E_C)$, i.e., the integral cross section summed over all final product states of the reaction versus the translational collision energy E_C , provides a measure of the total reactivity of the collision. The $\sigma_R(E_C)$ for $H^+ + D_2(\nu=0, j=0) \rightarrow HD + D^+$ is presented in Fig. 2 for the energy range 0.124–1.424 eV. We can see that the excitation function on the KBNN-PES decreases monotonically with the increasing collision energy within the energy range considered. An examination of the reactive classical trajectories reveals that the reaction proceeds through a capture process where the orbits pass the centrifugal barrier into a long-lived collision complex region. If the reactive cross section is decomposed into a capture cross section and a statistical transmission coefficient into the product channels, $\sigma_R = \kappa \sigma_C$, a Langevin model can be easily constructed based on the

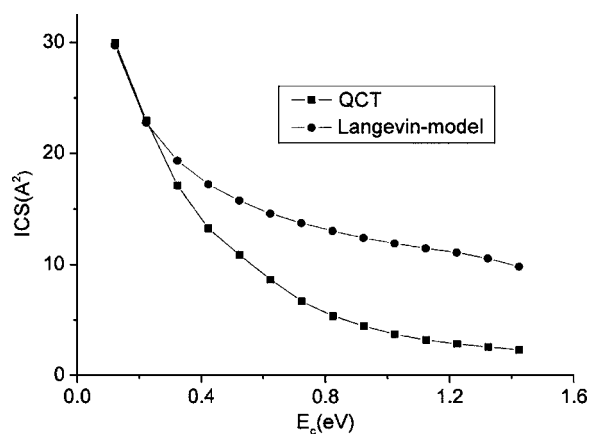


FIG. 2. The total integral cross section (excitation function) for the reaction $\text{H}^+ + \text{D}_2(\nu=0, j=0) \rightarrow \text{HD}(\nu'=\text{all}, j'=\text{all}) + \text{D}^+$ on the KBNN-PES as a function of collision energy. The solid curve is the result of the QCT simulation and the symbols denote the prediction of the Langevin model with a constant transmission coefficient.

KBNN-PES along the reaction path. Using a constant value for κ , we see in Fig. 2 that a fair model of the $\sigma_R(E_C)$ is obtained using elementary ideas.

The energy disposal of the reaction is likewise consistent with a statistical view of the breakup of an ion-molecule complex. In Fig. 3, the product translational energy (E_T) distribution, $P(E_T) = d\sigma/dE_T$, is exhibited for four collision energies. The distributions show a broad peak at low E_T followed by a decline at higher E_T as the internal product state density decreases.

The total differential cross section (DCS) (final-state summed) at four different collision energies, 0.224, 0.524, 1.024 and 1.424 eV, are displayed in Fig. 4. We define the c.m. scattering angle, θ , to be the angle between the outgoing vector of the D^+ product and the incident vector of the diatomic molecule D_2 . The QCT results show forward-backward peaking of the distribution that is roughly symmetrical. This is entirely consistent with the notion that the reaction proceeds through a complex that survives longer

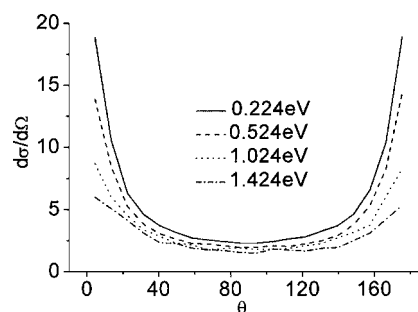


FIG. 4. Center-of-mass total (final-state summed) differential cross section for $\text{H}^+ + \text{D}_2(\nu=0, j=0) \rightarrow \text{D}^+ + \text{HD}$ at 0.224, 0.524, 1.024, and 1.424 eV in $\text{Å}^2/\text{sr}$. The scattering angle is defined as the angle between the incident D_2 beam and the D^+ product.

than the mean rotational period. The forward-backward peaking become more pronounced at low collision energies indicating a trend toward longer complex lifetimes as energy decreases.

The final-state-resolved DCSs for $\text{H}^+ + \text{D}_2(\nu=0, j=0) \rightarrow \text{HD}(\nu', j') + \text{D}^+$ are plotted versus (θ, j') in Fig. 5 at $E_C = 0.124, 0.224, 0.524$, and 1.024 eV. At the lowest two energies, only the $\nu'=0$ vibrational channel is open. At the higher two energies, the $\nu'=1$ state is allowed but the $\nu'=1$ results are shown only at the highest energy since for 0.524 eV the $\nu'=1$ production is very small. The results depicted in the figure make use of the Gaussian binning procedure for the final-state determination. It is seen that each final state exhibits the forward/backward peaking that was observed for the total DCS. The DCS generally varies smoothly as a function of j' although some fluctuations become more pronounced at higher energy. Much of this fluctuation is due to the decrease in reactivity at higher energy and, thus, the degradation in the statistical sampling. We suspect that these distributions will smooth out if more trajectories are used. For the $\nu'=0$ case, the j' distributions exhibit a single broad peak near $j'=3-5$. The $\nu'=1$ products, on the other hand, are clearly more rotationally hot. The finer details of the

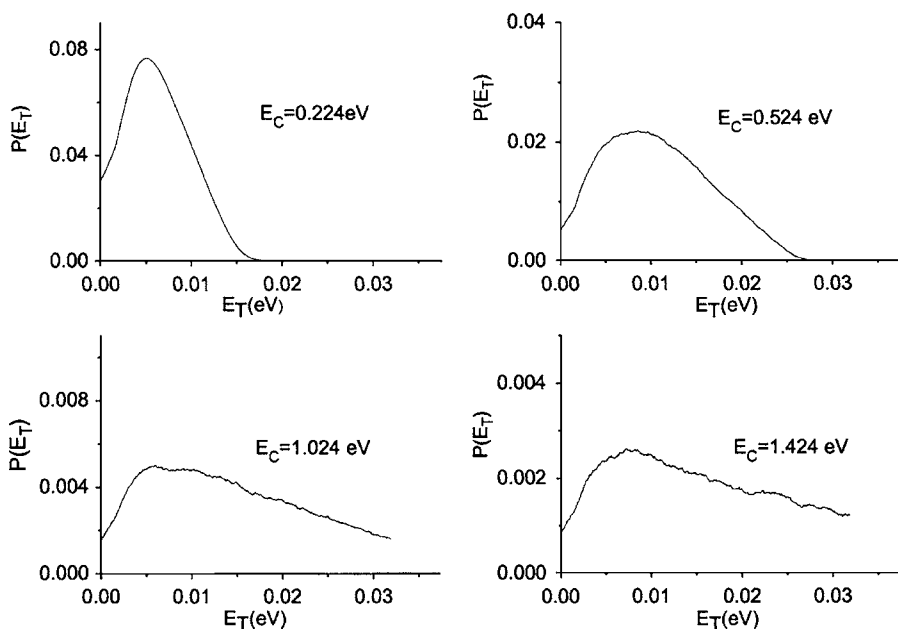


FIG. 3. Product translation energy distribution for the reaction $\text{H}^+ + \text{D}_2(0,0) \rightarrow \text{D}^+ + \text{HD}$ at four different collision energies.

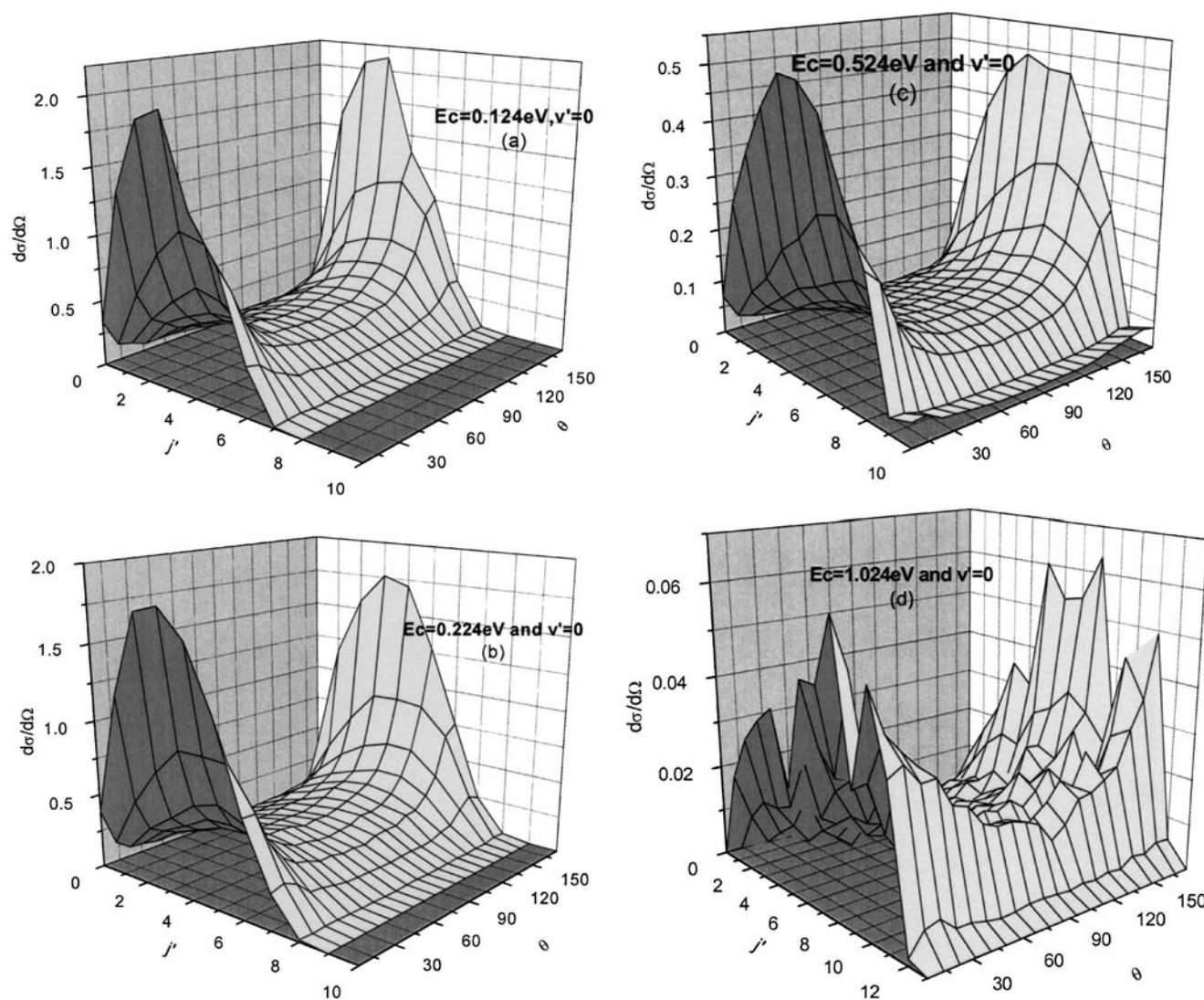


FIG. 5. The state-specific DCS in $\text{\AA}^2/\text{sr}$ at different collision energies for $\text{H}^+ + \text{D}_2(0,0) \rightarrow \text{D}^+ + \text{HD}(\nu', j')$ obtained from QCT with the Gaussian binning method. (a) $E_c = 0.124$ eV ($\nu' = 0$), (b) $E_c = 0.224$ eV ($\nu' = 0$), (c) $E_c = 0.524$ eV ($\nu' = 0$), and (d) $E_c = 1.024$ eV ($\nu' = 0, 1$).

results are found to depend somewhat on the specifics of the final-state binning procedure but the overall behavior of the cross sections are not overly sensitive.

Finally, it was possible to carry out a lifetime analysis of the complex forming trajectories that may prove useful in future work. In Fig. 6(a), we show a typical distribution of collision lifetimes obtained from Eq. (4) for the full ensemble of reactive trajectories computed at $E_c = 0.524$ eV. The linear distribution on the log-linear plot is a clear evidence for an exponential lifetime distribution that is expected from simple statistical theories.²⁹ The lifetime obtained at this energy was found to be 1.928 ps. Of course, the lifetimes are expected to depend on the angular momentum (J) of the complex since this quantity affects the height of the centrifugal barrier in the exit channel. In Fig. 6(b), we show the lifetime distributions obtained for various values of the impact parameter (and hence of J). Each distribution is exponential, although the lifetimes grow significantly with increasing J . The total lifetime for the full scattering problem is naturally dominated by the higher J contribution. The complex lifetimes also grow as the collision energy de-

creases. In Fig. 7, the $J=0$ lifetime is seen to increase significantly as the threshold is approached in agreement with conventional ideas of unimolecular decay.

IV. COMPARISON TO EXPERIMENTAL RESULTS

The central focus of the present study is the comparison of the QCT model for the ion-molecule reaction to the experimental results. First, we consider the direct comparison to the $\text{H}^+ + \text{D}_2$ scattering results obtained using an ion-beam experiment.^{18,17} At a collision energy of 0.52 eV, the time-of-flight product spectrum was measured at a laboratory scattering angle of 5° . The spectrum was then numerically fitted to a final product state distribution for $\text{HD}(\nu' j')$. Up to an overall scaling factor, this measurement reflects the state-resolved DCS at the c.m. scattering angles in the range of 10° – 25° . While the $\nu' = 1$ channel is open at this energy, vibrationally excited products were not detected, which is consistent with the very low $\nu' = 1$ DCS obtained in the QCT calculations. The $\text{HD}(\nu' = 0, j')$ rotational product distribution obtained is shown in Fig. 8. Superimposed on the plot is

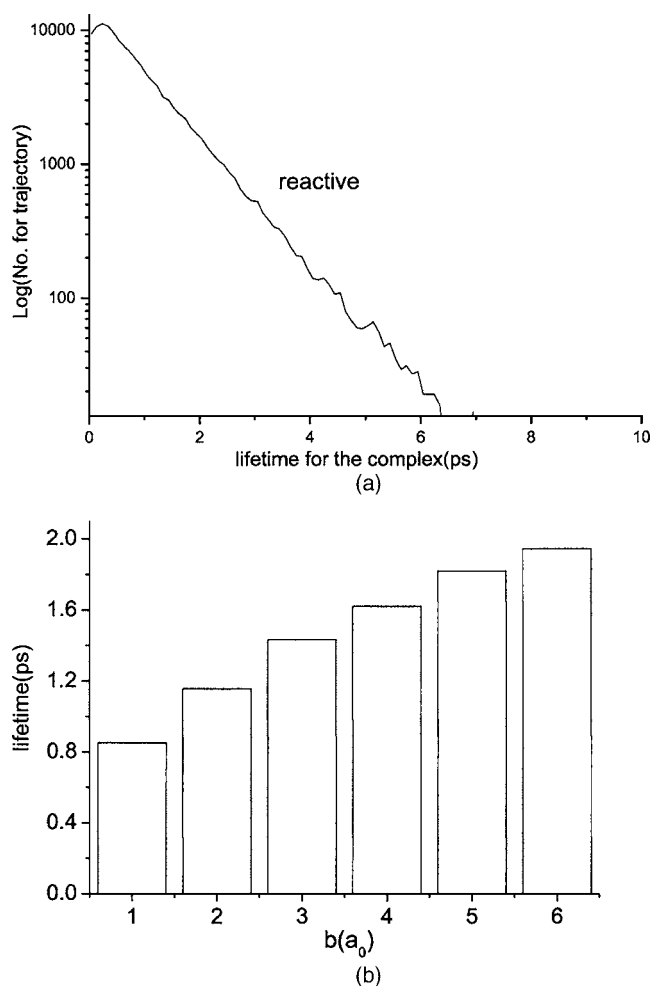


FIG. 6. (a) The collision time distribution for the reaction $H^+ + D_2 \rightarrow D^+ + HD$ at $E_c = 0.524$ eV computed using all reactive trajectories. The fitted lifetime is 1.928 ps. (b) The impact parameter (b) fixed (and hence J fixed) collision lifetimes obtained by fitting the lifetime distribution of $b = \text{constant}$ classical ensembles.

the corresponding QCT prediction based on the state-resolved DCS. It is seen that the QCT predictions are reasonably close to the results of the experiment and we view the agreement as evidence for the validity of the QCT model. Both exhibit a unimodal distribution peaking near $j' = 5$ or 6. The experimental results have been multiplied by a constant scaling factor to facilitate the comparison. In the lower panel

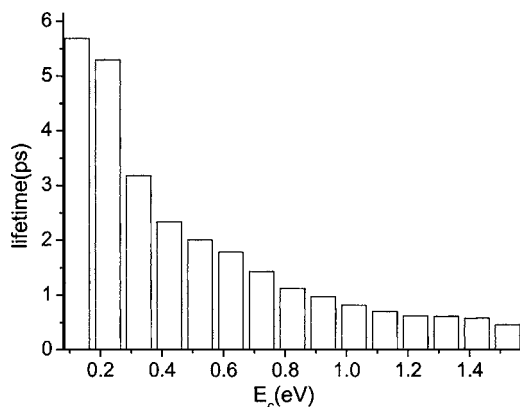


FIG. 7. Energy dependence of the fitted collision lifetimes at $J=0$.

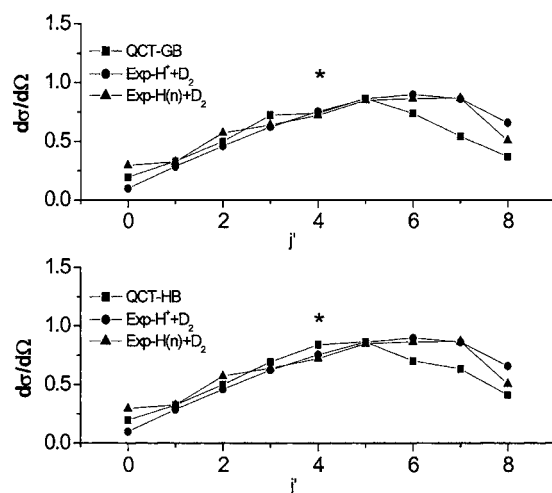


FIG. 8. A comparison of the product rotational number distribution between the experimental and QCT results at a special scattering angle (laboratory angle = 5°). In the upper panel the QCT results are obtained from the Gaussian binning method, while in the lower panel the QCT results are obtained from the histogram binning method.

of Fig. 8, the QCT results obtained from conventional histogram binning are plotted along with the experimental results. A modest improvement is noted when using the Gaussian binning method.

The data available¹⁷ for the RA reaction, $H(n) + D_2(0,0) \rightarrow D(n') + HD(\nu' j')$, are more extensive than for the direct ion-molecule reaction. It was possible to measure the rovibrational-state-resolved DCS at a large number of scattering angles using a $H(n)$ beam with $n=45$ and an extremely cold o - D_2 -molecule beam, hence $D_2(\nu=0, j=0)$. The final electronic quantum numbers, however, were not measured. As we have discussed in a previous report,¹⁷ the results of the RA reaction are in good agreement with the single ion-beam measurement. In Fig. 9, the time-of-flight

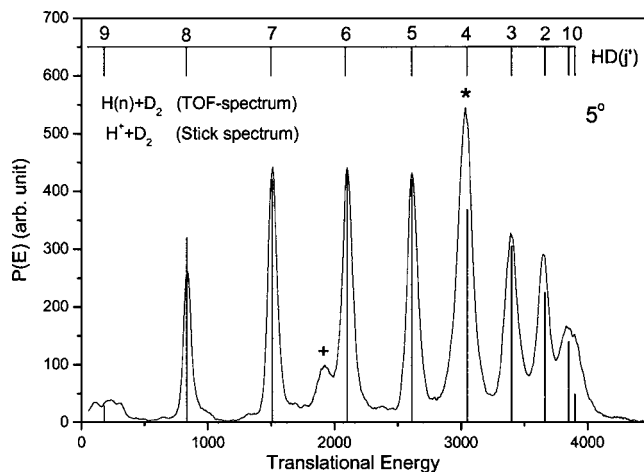


FIG. 9. Experimental product rotational distributions (see Ref. 17). The broadened spectrum is the TOF distribution (expressed as product translational energy in wavenumbers) measured for the $H(n) + D_2 \rightarrow D(n) + HD(\nu=0, j')$ reaction at the laboratory angle of 5° at $E_c = 0.524$ eV. The stick spectrum is the fitted distribution obtained for $H^+ + D_2 \rightarrow D^+ + HD(\nu=0, j')$ reaction at the laboratory scattering angle of 5° at $E_c = 0.524$ eV. The peak denoted by * for the RA spectrum is contaminated by the inelastic $H(n) + D_2 \rightarrow H(n') + D_2(\nu'=0, j'=10)$ channel. The peak with + is assigned to the $H(n') + D_2(\nu'=0, j'=11)$ channel.

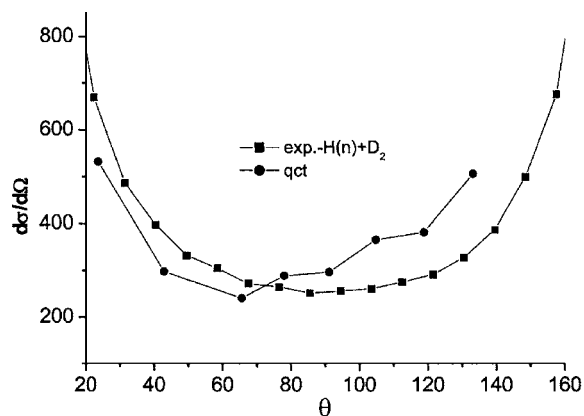


FIG. 10. The total (final-state summed) DCS vs c.m. scattering angle obtained from the experiment and QCT.

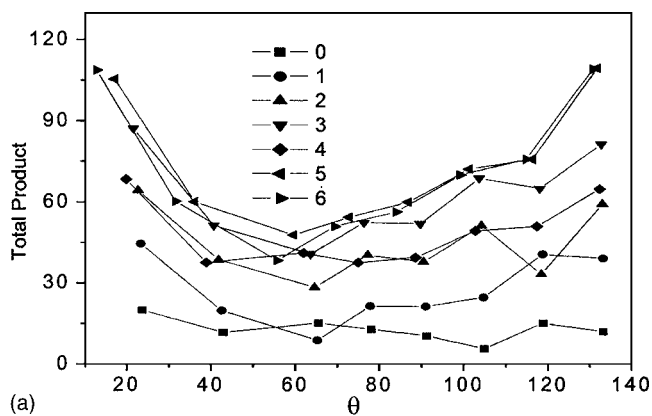
spectra for the two experiments are shown together. (The ion-beam results are shown with a stick spectrum.) The inferred rotational product distributions are quite similar, with the exception of the starred peak corresponding to the $D(n') + HD(0,4)$ product state. As we have discussed previously, it is likely that this peak is too high because the time-of-flight (TOF) spectrum is contaminated by a contribution from the $H(n) + D_2(0,0) \rightarrow H(n) + D_2(v'=0, j'=10)$ state that occurs at the same position. When inelastic scattering contribution is subtracted from the intensity for this peak, as illustrated in Fig. 8, the j' distribution for the RA experiment becomes remarkably similar to the ion-beam experiment.

In Fig. 10, the total (state summed) reactive DCS at 0.524 eV obtained from the RA experiment is plotted versus the c.m. scattering angle. Also shown is the QCT prediction interpolated to the experimental scattering angles. Qualitatively, the distributions are similar. However, it is apparent that the experimental DCS is somewhat more asymmetrical (forward versus backward) than the QCT prediction. It is possible that a fully quantum treatment of the dynamics may assuage this discrepancy, however, our view is that this is unlikely. In Fig. 11(a), the experimental final-state-resolved DCSs are plotted versus θ for $j'=0-6$ at $E_c=0.524$ eV. Each state exhibits forward-backward peaking but also exhibits some fluctuations versus the scattering angle. We expect that the magnitude of those fluctuations provides a sense of experimental error bars. The QCT results, plotted in Fig. 11(b), are again similar to the experimental results. The j' ordering of the magnitude of the QCT-DCS is roughly the same as the experiment as is the independence of that ordering from the scattering angle.

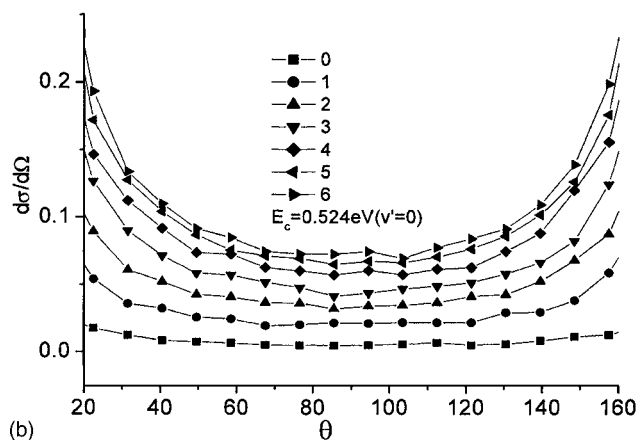
While the QCT results are not perfect, it is clear that agreement with the experiment is reasonably good. Given the expected errors in the PES and the neglect of quantum effects in the scattering calculations, we conclude that the simulations tend to confirm the view that the RA reaction proceeds through an ion-molecule collision consistent with the Fermi independent-collider model.

V. THE ROLE OF THE RYDBERG ELECTRON

The potential influence of the “spectator” Rydberg electron on the reaction dynamics is an important practical issue



(a)

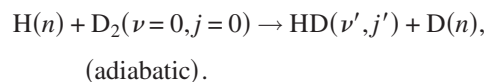


(b)

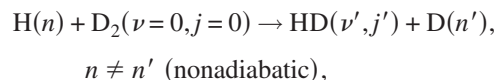
FIG. 11. The final-state-specific DCS angular distribution for a number of $HD(v'=0, j')$ product states at $E_c=0.524$ eV. In (a), the experimental results for the reaction $H(n) + D_2 = D(n) + HD(v'=0, j')$, while in (b) is the QCT results for the reaction $H^+ + D_2 = D^+ + HD$. The contamination of the $j'=4$ experimental result due to the overlapping inelastic channel has been corrected through a numerical estimation of the size of the two contributions.

for the interpretation of the experimental results as well as a fascinating problem in theoretical dynamics. An in-depth treatment of the nonadiabatic dynamics is beyond the scope of the present work, but nevertheless we can make some remarks on this problem based on elementary models.

In the simplest view of the collision, the Rydberg state of the electron is totally unaffected by the collision and reaction is electronically adiabatic,



Since the initial and final Rydberg energies are nearly equal in this case, the TOF spectra obtained can be solely assigned to the final rovibrational states of the product molecule. In the more general nonadiabatic case,



electronic energy transfer can shift or broaden the rovibration TOF spectrum. At $n=45$, the Rydberg level spacing is 0.2 meV while the ionization energy is only 5 meV. By comparison, the thermal beam spread in molecular-beam collision energy is about 11 meV which is the main underlying

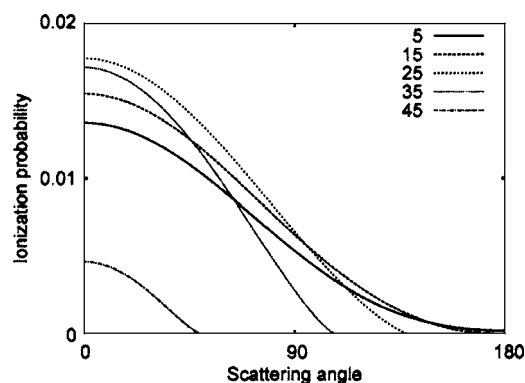


FIG. 12. Ionization probability for $H(n=50, 1)$ computed from the classical impulse approximation as a function of the c.m. scattering angle for various l values. The results are obtained by averaging Eq. (5) over the phase of the Bohr orbit and the orientation of the Rydberg state. The $n=50$ is an upper bound to the principle quantum number employed in our experiments to date and the ionization is lower for smaller values of n . The scattering angle of 0 corresponds to backward (rebound) scattering of the positive charge carrier.

source of the peak width in the TOF spectrum, such as shown in Fig. 9. Thus, unless Δn of the collision is extremely large, the electronic energy transfer should have little influence on the measured TOF peak positions or widths. The absence of any noticeable peak shifts or significant increase in the peak widths for the RA+molecule reaction compared to the ground-state reaction, $H(n=0)+D_2$, measured using the same apparatus previously,^{30,31} provides direct experimental evidence that Δn is, in fact, not particularly large.

While the extent of inelastic electronic energy transfer is apparently not too large, it does not necessarily follow that the collision dynamics is unaffected by the Rydberg-electron nor that Eq. (3) must hold. A variety of scenarios is consistent with the experimental results. For example, if the initial (final) diatom should undergo a secondary collision with the Rydberg electron in addition to the primary ion-core scattering, near-resonant energy transfer with the rotational diatomic states could occur which would modify Eq. (3). Free-electron scattering models have previously been introduced to estimate the collision cross sections for such rotationally inelastic processes. Based on those models, the cross sections for rotationally inelastic scattering should be on the order of $10\text{--}50 \text{ \AA}^2$.³² On the hand, the electron “target” is distributed on a sphere of radius $r_n \sim 2000 \text{ \AA}$. The ratio of the cross section to the area of the sphere provides a crude estimate of the probability for a reactive (i.e., ion-core) collision to undergo a secondary collision. Clearly the resulting ratio of <0.001 suggests that two such collision processes are unimportant.

A much more subtle issue concerns electronically nonadiabatic processes that may affect the product detection in the experiment. The DCS is measured by the field ionization of the RA arriving at the microchannel plate (MCP) detector. Should the RA ionize or decay to a low n -level before arrival at the detector, it simply will not be measured. The RA must survive on the order of tens of microsecond to complete the time-of-flight experiment. It is well known that the lifetime of the RA is extremely sensitive to the l -quantum number and scales roughly as $n^3 l^2$ for high-lying states.^{33,34} Indeed,

Schneider *et al.*¹⁵ found it necessary to use external fields in the generation of RA to guarantee sufficiently large l , and thus long enough lifetimes, to complete the experiment (our experiments rely on the same techniques¹⁶). Thus, we must consider whether the reactive collision will induce ionization or transitions to low- l states that spontaneously emit.

While a sophisticated treatment of the electronically nonadiabatic dynamics (using, e.g., quantum defect theory³⁵) is beyond our scope, we can make some elementary observations based on our classical model. The direct ionization rate of the Rydberg electron can be viewed as the sum of two contributions. First, there is the impulsive change in the velocity of the positive charge carrier due to the kinematics of the collision. A simple estimate of the final RA energy using classical mechanics is

$$E_f = \frac{(\mathbf{p} + \Delta\mathbf{p})^2}{2} - \frac{1}{r}, \quad (5)$$

where $\Delta\mathbf{p}$ is the momentum transfer of the positive charge in the original rest frame of the RA and a distribution of E_f is obtained by sampling over the Bohr orbit. Since Eq. (5) depends on the scattering angle, this ionization probability could attenuate the observed signal as a function of θ . As shown in Fig. 12, the results of Eq. (5) for $E_f > 0$ under the most severe conditions of the present experiments show a maximal effect of less than 2%. While not negligible, the influence is probably below the experimental error bars. The second source of ionization is vibrational autoionization of the long-lived collision complex. Since the ionization probability (P_I) is expected to follow the relation $P_I = w\tau$, where w is the ionization probability per unit time and τ is the lifetime, longer-lived complexes are naturally expected to suffer more autoionization. The autoionization is due to the coupling of the electron motion to the oscillating field produced by the vibration motions in the HD_2^+ complex. The ionization rate of the Rydberg atoms in oscillating external fields has been extensively studied, largely as a problem in quantum chaos. Based on the dramatic fall off of the ionization rate with increasing frequency and weak time-dependent coupling of the ionic core to the distant electron, we conjecture that the autoionization rate may be low except for extremely long-lived complexes.³⁶

Finally, we note that collision-induced $l \rightarrow l'$ ($l > l'$) transitions may attenuate the measured signal due to the increased rate of spontaneous emission of low-lying l' levels of the RA. Again using the simple classical impulse approximation, we estimate that the change in angular momentum of the electron might be quite large, $|\Delta\mathbf{p} \times \mathbf{r}|$. Since $|\Delta\mathbf{p}| \sim 0.01 \text{ a.u.}$ and $|\mathbf{r}| \sim 2000 \text{ a.u.}$ the l' levels of the RA could potentially be completely mixed³⁷ and the signal attenuated by the statistical fraction of rapidly emitting states (perhaps 10%). Of course the net result of this process upon the measured DCS depends on the *difference* of emission rates when varying the scattering angle and final state since the overall scaling of the signal is arbitrary. Obviously, a more detailed treatment of this intricate dynamics and the subsequent emission kinetics is required before any conclusions can be reached.

VI. CONCLUSIONS

We have studied the $H(n)+D_2 \rightarrow HD+D(n')$ chemical reaction using a simple theoretical model. Our motivation was the outcome of a recent experimental study that discovered that the collision dynamics of $H(n)+D_2 \rightarrow HD+D(n')$ was remarkably similar to those observed for the ion-molecule reaction $H^++D_2 \rightarrow HD+D(n')$. However, the comparison of the two systems was limited in that only a single scattering angle had been measured for the ion-molecule reaction. Therefore, we carried out QCT calculations on the ion-molecule reaction to facilitate a more complete comparison to the RA reaction. Should it be found that RA+molecule and ion+molecule were, in fact, equivalent it would prove to be of great practical significance for the high-resolution study of ion-molecule reactions.

The results of the QCT calculations were completely consistent with the usual expectations for simple ion-molecule reactions. The reaction was found to proceed through a long-lived collision complex that decays exponentially in time. The lifetime was sufficiently long to yield a roughly symmetrical forward-backward peaking product distribution. The final rotational product distribution was smooth and unimodal (when the trajectory statistics was sufficient). The details of the implementation of the initial/final-state semiclassical quantization conditions had a relatively small effect on the results, although as noted earlier the use of Gaussian binning of the product states gives somewhat better agreement with the experiment.

The comparison of the QCT results to the experimental measurements for $H(n)+D_2 \rightarrow HD+D(n')$ seems to generally support the proposition that the reaction proceeds through the ion-molecule mechanism. The product rotational state distributions were found to be well reproduced by QCT. Furthermore, these state distributions were roughly independent of scattering angle (aside from some fluctuations in the experimental DCS) for both theory and experiment. The angular product distributions exhibited characteristic forward-backward peaking in both the experiment and QCT simulations. The most significant difference between theory and experiment was the appearance of a higher level of forward-backward asymmetry of the DCS in the experimental measurement. This disagreement needs to be addressed in future work since forward-backward symmetry is a generic feature of reactions proceeding through long-lived intermediates. Full quantum scattering calculations on the ion-molecule reaction will undoubtedly soon be possible for this system, and the potential influence of quantum effects will then be determined.

Finally, we considered the potential influence of the Rydberg electron on the underlying ion-core+molecule scattering. Based on simple order-of-magnitude estimates, it was concluded to be unlikely that the electron could significantly modify the nuclear dynamics. The absence of broadening of experimental TOF spectral peaks provided direct evidence for this conclusion. However, we identified the issue of experimental signal attenuation as a key point for the practical validity of Eq. (3), i.e., the equivalence of the ion+molecule and RA+molecule DCS. Should the Rydberg

electron ionize or emit during the course of the RA experiment, then the measured signal may be affected in a state- and angle-dependent fashion. If this occurs, then sophisticated "instrument functions" would be required to make use of Eq. (3). Clearly, this matter requires further theoretical work.

As a final note, after the completion of this work we have become aware of the newly published work by Wrede *et al.*³⁸ that also experimentally investigates the reaction of Rydberg atoms in a molecular-beam experiment. We encourage interested readers to see Ref. 38.

ACKNOWLEDGMENTS

This work was supported by the Chinese Academy of Science of China, the National Science Council of Taiwan, National Natural Science Foundation of China, and Academia Sinica of Taiwan.

- ¹M. Matsuzawa, in *Rydberg States of Atoms and Molecules*, edited by R. F. Stebbings and F. B. Dunning (Cambridge University Press, Cambridge, 1983).
- ²T. F. Gallagher, *Rydberg Atoms* (Cambridge University Press, Cambridge, 1994).
- ³M. Matsuzawa, in *Rydberg States of Atoms and Molecules*, edited by R. F. Stebbings and F. B. Dunning (Cambridge University Press, Cambridge, 1983), p. 267.
- ⁴E. Fermi, *Nuovo Cimento* **11**, 157 (1934).
- ⁵C. A. Kocher and A. J. Smith, *Phys. Rev. Lett.* **39**, 1516 (1977).
- ⁶J. Boulmer, G. Baran, F. Devos, and J.-F. Felpech, *Phys. Rev. Lett.* **44**, 1122 (1980).
- ⁷P. M. Koch, *Phys. Rev. Lett.* **43**, 432 (1979).
- ⁸L. J. Wang, M. King, and T. J. Morgan, *J. Phys. B* **119**, L623 (1986).
- ⁹M. R. Flannery, *Ann. Phys. (N.Y.)* **61**, 465 (1970).
- ¹⁰M. Matsuzawa, *J. Chem. Phys.* **55**, 2685 (1971); **58**, 2674(E) (1973).
- ¹¹G. N. Foulmer and T. W. Preist, *J. Chem. Phys.* **56**, 1601 (1972).
- ¹²B. S. Strazisar, C. Lin, and H. F. Davis, *Phys. Rev. Lett.* **86**, 3997 (2001).
- ¹³X. Ling, B. G. Lindsay, K. A. Smith, and F. B. Dunning, *Phys. Rev. A* **45**, 242 (1992).
- ¹⁴S. T. Pratt, J. L. Dehmer, P. M. Dehmer, and W. A. Chupka, *J. Chem. Phys.* **101**, 882 (1994).
- ¹⁵L. Schneider, K. Seekamp-Rahn, E. Wrede, and K. H. Welge, *J. Chem. Phys.* **107**, 6175 (1997).
- ¹⁶S. D. Chao, S. A. Harich, D. X. Dai, C. C. Wang, X. Yang, and R. T. Skodje, *J. Chem. Phys.* **117**, 8341 (2002); G. Wu, Q. Ran, D. Dai, and X. Yang, *ibid.* (to be published).
- ¹⁷D. Dai, C. C. Wang, G. Wu, S. A. Harich, H. Song, M. Hayes, R. T. Skodje, D. Gerlich, and X. Yang, *Phys. Rev. Lett.* **95**, 013201 (2005).
- ¹⁸D. Gerlich, Dissertation, Faculty of Physics, University of Freiburg, May 1977.
- ¹⁹V. G. Ushakov, K. Nobusada, and V. I. Osherov, *Phys. Chem. Chem. Phys.* **3**, 63 (2001).
- ²⁰I. Last, M. Gilibert, and M. Baer, *J. Chem. Phys.* **107**, 1451 (1997).
- ²¹A. N. Panda and N. Sathyamurthy, *J. Chem. Phys.* **122**, 054304 (2005).
- ²²I. G. Csizmadia, J. C. Polanyi, A. C. Roach, and W. H. Wong, *Can. J. Chem.* **47**, 4097 (1969).
- ²³D. Gerlich, *J. Chem. Phys.* **92**, 2377 (1989).
- ²⁴H. Kamisaka, W. Bian, K. Nobusada, and H. Nakamura, *J. Chem. Phys.* **116**, 654 (2002).
- ²⁵D. L. Bunker, *Methods Comput. Phys.* **10**, 287 (1971).
- ²⁶D. G. Truhlar and J. T. Muckerman, in *Atom-Molecule Collision Theory: A Guide for Experimentalists*, edited by R. B. Bernstein (Plenum, New York, 1979).

- ²⁷L. Bonnet and J. C. Rayez, *Chem. Phys. Lett.* **227**, 183 (1997).
- ²⁸L. Banares, F. J. Aoiz, P. Honvault, and J. M. Launay, *J. Phys. Chem. A* **108**, 1616 (2004).
- ²⁹R. G. Gilbert and S. C. Smith, *Theory of Unimolecular and Recombination Reactions* (Blackwell, Boston, 1990).
- ³⁰S. A. Harich, D. Dai, C. C. Wang, X. Yang, S. D. Chao, and R. T. Skodje, *Nature (London)* **419**, 281 (2002).
- ³¹D. Dai, C. C. Wang, S. A. Harich, X. Wang, X. Yang, S. D. Chao, and R. T. Skodje, *Science* **300**, 1730 (2003).
- ³²M. R. Flannery, *Ann. Phys. (N.Y.)* **79**, 480 (1973).
- ³³M. R. Flannery and D. Vrinceanu, *Phys. Rev. A* **68**, 030502(R) (2003).
- ³⁴S. D. Chao, S. H. Lin, H. L. Selzle, and E. V. Schlag, *Chem. Phys. Lett.* **265**, 445 (1997).
- ³⁵V. Kokoouline and C. H. Greene, *Phys. Rev. A* **68**, 012703 (2003).
- ³⁶W. A. Chupka, *J. Chem. Phys.* **98**, 4520 (1993).
- ³⁷S. D. Chao and S. H. Lin, *Chin. J. Phys. (Taipei)* **37**, 442 (1999).
- ³⁸E. Wrede, L. Schnieder, K. Seekamp-Schieder, B. Niederjohann, and K. H. Welge, *Phys. Chem. Chem. Phys.* **7**, 1577 (2005).